Available online at www.sciencedirect.com
SCIENCE DIRECT®
European Journal of Medicinal Chemistry 39 (2004) 153–160
EUROPEAN JOURNAL OF MEDICINAL CHEMISTRY
www.elsevier.com/locate/ejmech

Original article

Synthesis of 1-(2-chloro-2-phenylethyl)-6-methylthio-1*H*-pyrazolo[3,4-*d*]pyrimidines 4-amino substituted and their biological evaluation

Silvia Schenone [a,*], Olga Bruno [a], Francesco Bondavalli [a], Angelo Ranise [a], Luisa Mosti [a], Giulia Menozzi [a], Paola Fossa [a], Fabrizio Manetti [b], Lucia Morbidelli [c], Letizia Trincavelli [d], Claudia Martini [d], Antonio Lucacchini [d]

[a] *Dipartimento di Scienze Farmaceutiche, Università degli Studi di Genova, viale Benedetto XV, 16132 Genoa, Italy*
[b] *Dipartimento Farmaco Chimico Tecnologico, Università degli Studi di Siena, via Aldo Moro, 53100 Siena, Italy*
[c] *Dipartimento di Biologia Molecolare, Università degli Studi di Siena, via Aldo Moro, 53100 Siena, Italy*
[d] *Dipartimento di Psichiatria, Neurobiologia, Farmacologia e Biotecnologie, Università degli Studi di Pisa, via Bonanno, 56126 Pisa, Italy*

Received 12 June 2003; received in revised form 19 November 2003; accepted 19 November 2003

Abstract

A new series of 4-amino-6-methylthio-1*H*-pyrazolo[3,4-*d*]pyrimidines (**2a–m**) bearing the 2-chloro-2-phenylethyl chain at the N1 position, has been synthesized. The affinity of these compounds for A_1 adenosine receptor (A_1AR) was measured. The compounds showed poor affinity. A more interesting result was obtained by **2a, 2d, 2g**, which demonstrated inhibitory activity on cell proliferation of the A-431 cell line stimulated by epithelial growth factor (EGF) and on EGF receptor tyrosine kinase (EGFR-TK) phosphorylation.

Keywords: Pyrazolo-pyrimidines; Adenosine; Epidermal growth factor

1. Introduction

Adenosine is an endogenous neuromodulator, which mediates its biological effects by interacting with four receptor subtypes named A_1, A_{2A}, A_{2B}, and A_3, identified and cloned from various mammalian tissue types [1–3].

Despite the large number of potential therapeutic applications, relatively few compounds have entered into clinical trials and are used in the clinic [4,5]. This fact is also due to the poor selectivity of inhibitors for unique adenosine receptor subtype. Consequently, there has been an expanded interest in finding selective molecules that lack undesirable side effects.

In recent years, a wide variety of nitrogen-containing heterocycles have been synthesized as possible A_1 selective antagonists [6,7]. In particular, among these, pyrazolo[3,4-*b*]pyridine [8,9] and pyrazolo[3,4-*d*]pyrimidine [10–13] derivatives were found to be selective ligands with antagonist activity for A_1 adenosine receptors (A_1AR). They may have therapeutical use as cognitive enhancers, anti-dementia drugs (e.g. for Alzheimer's disease and cerebrovascular dementia), psycostimulants, anti-depressant drugs and ameliorants of cerebral function [14]. A_1AR antagonists have also demonstrated promising therapeutic potential for renal and cardiac failure [15,16].

We recently synthesized a series of 4-amino-1-(2-chloro-2-phenylethyl)-1*H*-pyrazolo[3,4-*b*]pyridine-5-carboxylic acid ethyl ester derivatives **1** [17] (see Fig. 1). The affinity data showed that these new molecules bind the A_1AR in a completely selective way. Some of the compounds show interesting affinity and antagonistic activity.

In order to find a more active and A_1 selective antagonist, we recently developed a pseudoreceptor model [18] (constructed taking into consideration structure–activity data of molecules derived both from our own research and also collected from current literature) capable of predicting the A_1 binding activity of compounds not yet synthesized.

* Corresponding author.
E-mail address: schensil@unige.it (S. Schenone).

doi:10.1016/j.ejmech.2003.11.007

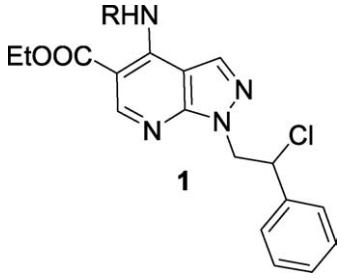

Fig. 1

Based on this theoretical model and taking into account that the SAR data evidenced both the 2-chloro-2-phenylethyl group in position 1 of the pyrazole ring and the substituted nitrogen at the 4 position of the pyridine nucleus as important features for activity of compounds **1** toward A_1AR, we envisaged the family of 1-aryl-4-amino substituted-6-methylthio-1*H*-pyrazolo[3,4-*d*]pyrimidine derivatives **2**, as an attractive field of investigation. These new compounds share a heterocyclic structure more strictly isosteric to the purinic moiety of adenosine and appear as interesting compounds to be synthesized and tested as A_1AR inhibitors. In fact, binding activity of the N4 propyl, butyl, and cyclopropyl derivatives were predicted by the pseudoreceptor model to be 13, 2, and 160 nM, respectively. Moreover, it is worth pointing out that 6-thio-substituted pyrazolo[3,4-*d*]pyrimidines that show an excellent activity against A_1AR, are already present in current literature [19,20].

2. Chemistry

The synthetic route to the target compounds is outlined in the Scheme 1.

The starting material is ethyl ester of 5-amino-1-(2-hydroxy-2-phenylethyl)-1*H*-pyrazole-4-carboxylic acid (**3**), obtained following our reported procedure [18]. Reaction of **3** with benzoyl isothiocyanate in THF at reflux for 8 h yielded the intermediate **4**. Cyclization to the pyrazolo[3,4-*d*]pyrimidine intermediate **5** was achieved by treating **4** with 1 M NaOH at 100 °C for 10 min, followed by acidification with acetic acid (80% yield). Alkylation of **5** with methyl iodide in THF at reflux afforded the 6-thiomethyl derivative **6**. The latter was in turn treated with the Vilsmeier complex ($POCl_3$:DMF) to obtain the dihalogenated compound **8** bearing the chlorine atom either at position 4 of the pyrimidine nucleus and on the N1 side chain. Compound **8** was purified in good yield by chromatography on a Florisil® column.

It is interesting to point out that treatment of **6** with $POCl_3$ at reflux afforded the undesired product **7**, resulting from dehydrohalogenation of the N1 side chain.

Finally, regioselective substitution of the C4 chlorine atom with an excess of various amines afforded the desired compounds **2a–m** in yields ranging between 60% and 80%. Notably, the chlorine atom on the side chain was not substituted by the amine in spite of its benzylic position, as shown by the ^{1}H NMR chemical shifts of the CH_2–CH side chain, which give an ABX complex pattern owing to the non-equivalence of CH_2-protons.

3. Pharmacology

All the compounds were tested for their ability to displace [^{3}H]N6-cyclohexyladenosine ([^{3}H]CHA) from A_1AR and [^{3}H]-2-{[4-(2-carboxyethyl)phenylethyl]amino}-5-(*N*-ethylcarbamoyl) adenosine ([^{3}H]CGS21680) from A_{2A}AR in bovine cortical and striatal membranes, respectively [16]. The A_1 and A_{2A} receptor binding affinities for compounds **2a–m** (see Table 1), are expressed as K_i or % of inhibition of binding (at 10 μM compound concentration).

4. Result and discussion

This new family of 6-methylthio-pyrazolo[3,4-*d*]pyrimidines is evidently less active than the pyrazolo[3,4-*d*]pyridines synthesized by us and bearing the same 2-chloro-2-phenylethyl side chain on the N1 of the pyrazole ring. In fact, the most potent compounds in this series were **2a** and **2b** having the cyclopropylamino and *n*-propylamino group at the C4, showing A_1AR affinity of 0.5 and 0.9 μM, respec-

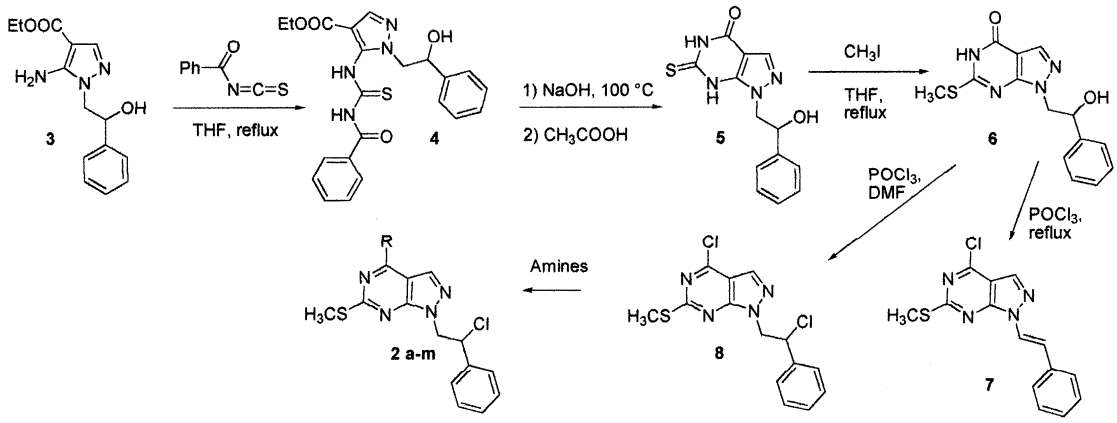

Scheme 1

Table 1
Binding activity of compounds **2a–m** at bovine A_1 and A_{2A} adenosine receptors

Compounds	R	A_1AR affinity (K_i or % inhibition at 10 μM) [a]	A_{2A}AR affinity (K_i or % inhibition at 10 μM) [a]
2a	NH cyclopropyl	0.52	60%
2b	NHC_3H_7	0.90	51%
2c	NHC_4H_9	2.08	34%
2d	$NHC(CH_3)_3$	15	25%
2e	$N(C_2H_5)_2$	11%	20%
2f	$NH(CH_2)_2OC_2H_5$	37%	37%
2g	NH cyclohexyl	5.84	19%
2h	1-Pyrrolidinyl	46%	6.7%
2i	1-Piperidinyl	34%	0%
2j	4-Morpholinyl	45%	19%
2k	1-Hexahydroazepinyl	28%	0%
2l	$NHCH_2C_6H_5$	18%	20%
2m	$NHCH_2CH_2C_6H_5$	9.44	2.6%

[a] The K_i values are mean ± S.E.M. of three separate assays, each performed in triplicate.

tively. Increasing the length or bulkiness of the side chain led to a significant decrease in affinity, the *n*-butyl (**2c**) and *tert*-butyl (**2d**) derivatives showing affinity values of 2 and 15 μM, respectively. The remaining compounds of the series were inactive, showing that a short and not too bulky side chain (*n*-propyl and cyclopropyl) on the C4 nitrogen atom is necessary for these ligands to bind A_1AR.

Based on these findings, several conclusions can be put forward. (i) The pharmacophore model developed by us to predict A_1 activity has to be revised according to the new results. Work in this direction is already ongoing. (ii) The presence of the ester moiety at C5 of **1** is necessary for the A_1AR activity, according to the suggestion that this group could give a profitable internal hydrogen bond with the NH at C4 [18]. (iii) Compounds lacking the C6 substituent show even lower A_1 affinity, suggesting the preparation of new derivatives with a longer chain at C6 [21].

Recently, Traxler et al. [22], on the basis of a pharmacophore model for inhibitors competing for the ATP-binding site of the epidermal growth factor receptor (EGFR), reported the design and synthesis of a potent and selective EGFR tyrosine kinase (EGFR-TK) inhibitor belonging to the 4-phenylaminopyrazolo[3,4-*d*]pyrimidine family. Moreover, the crystal structure of the kinase domain from EGFR has been determined at a 2.6 Å resolution, in complex with a 4-anilinoquinazoline inhibitor, erlotinib, currently in Phase III clinical trials as an anti-cancer agent [23]. Based on both these literature reports, we have performed molecular docking simulations using the crystallographic coordinates of EGFR as the input macromolecular target and the position of erlotinib into the EGFR-TK binding site to orient our molecules, with the purpose of ascertaining whether **2a–m** could interact profitably with EGFR.

It is important to note that in the present study, the computational step corresponding to the molecular docking approach is simplified, since the functional groups of inhibitors (i.e. erlotinib) interacting with the enzyme and the amino acid residues of the binding site are well known from X-ray. Thus, the docking problem is essentially reduced to locate the possible conformations of the new pyrazolo-pyrimidino derivatives within the active site of the enzyme.

All the complexes generated by docking simulations were then submitted to statistical conformational search with Monte Carlo Multiple Minimum (MCMM) method involving all the rotatable bonds of the ligand and following a computational protocol reported in detail in Section 6.

In a first attempt, the crystallographic coordinates of the 4-aminopyrimidine nucleus of erlotinib were used to drive the superposition of the corresponding ring of **2a** into the experimental EGFR-TK binding site. Such an orientation allowed us to find a hydrogen bond contact between the N7 atom of **2a** and the amide NH group of Met769 (Fig. 2), as previously described in the EGFR–erlotinib complex [23]. Upon minimization of this complex, a conformational rearrangement was found to force both Thr766 and Gln767 away from their original position and to eliminate steric clashes involving these amino acids and the thiomethyl group of the inhibitor. Such a structural reorganization led to complexes lacking all the hydrogen bonds involving the pyrimidine ring of **2a**, that on the basis of literature reports were considered as non-interesting complexes and consequently not further investigated.

On the other hand, a different orientation of **2a** (Fig. 3), corresponding to that proposed by Traxler for 1-aryl-pyrazolopyrimidines gave more interesting results. In fact,

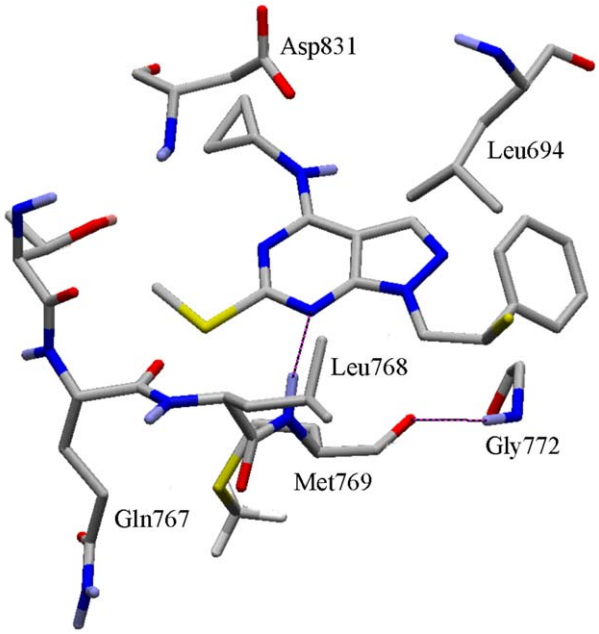

Fig. 2. Complex between compound **2a** and the EGFR-TK binding site, as obtained by superposition of the pyrazolo-pyrimidine derivative onto the crystallographic structure of the 4-aminopyridine nucleus of erlotinib. The N7 endocyclic nitrogen atom is at a hydrogen bond distance from the backbone amide group of Met769. For sake of clarity, only few amino acids of the macromolecule were displayed.

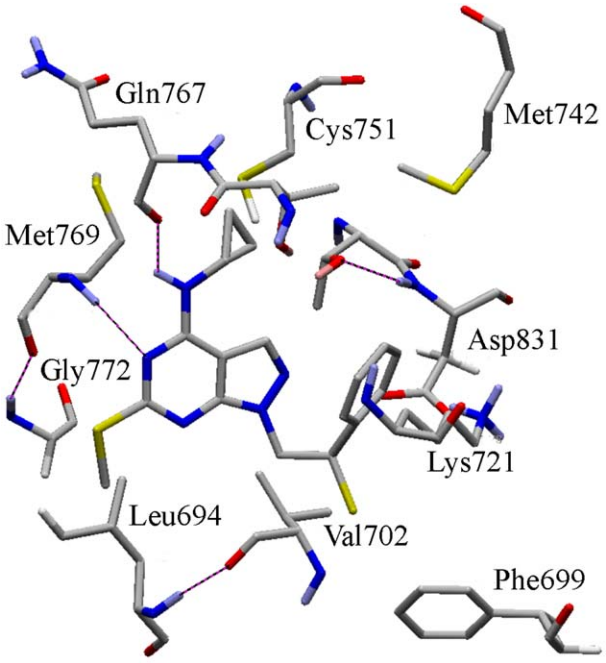

Fig. 3. Complex between compound **2a** and the EGFR-TK binding site, with the pyrazolo-pyrimidine derivative oriented in agreement with what proposed by Traxler. A bidentate hydrogen bond acceptor/donor system anchoring **2a** into the ATP binding site, was found, involving Met769 and Gln767 of the macromolecule and the N5 endocyclic nitrogen and the exocyclic amino nitrogen, respectively.

the N5 pyrimidine nitrogen atom together with the secondary amino group at the 4-position constitute the bidentate hydrogen bond acceptor–donor system anchoring **2a** within the ATP binding site of the EGFR. The corresponding receptor counterparts are represented by the NH amide backbone of Met769, and the carbonyl group of Gln767, respectively. According to this binding mode, the 2-chloro-2-phenylethyl side chain lies into a large pocket mainly defined by Phe699, Val702, Lys721, and Asp831. Moreover, the cyclopropyl ring is accommodated within a region constituted by three sulforated residues (namely, Met742, Cys751, and Met769) and two threonine amino acids (namely, 766 and 830), in addition to Leu820. Finally, the methylthio substituent at the 6-position is located into a region of the binding site (delimited by Leu694 and Gly772) where no profitable interaction with the macromolecule was found, similarly to some 6-amino derivatives reported by Traxler et al. [22].

The biological activity of **2a, 2d** and **2g** was assessed on A-431 cell line expressing EGFR. Proliferation and cytotoxicity [1] of A-431 cells and the autophosphorylation of EGFR in response to the three pyrazolo-pyrimidines, were evaluated. Compound **2a** tested at 50 nM in the presence of EGF inhibited cell proliferation by 40%. The known inhibitor of the EGFR, AG1478, showed similar inhibitory activity of cell proliferation (33%). Lower concentration of **2a** (10 nM) produced marginal inhibition of cell proliferation (10%), while a 1000-fold higher concentration (10 μM) provided the maximal effect. A similar trend was found for **2d** and **2g** when tested at the same concentrations. While a 10 μM concentration led to the maximal effect for both compounds, a 50 nM concentration produced a cell proliferation inhibition of 28% and 19%, respectively. Any significant anti-proliferative activity was found at 10 nM concentrations.

In cytotoxicity assay, a nanomolar concentration of **2a** was not effective, while a higher concentration (10 μM) produced significant cell death (36%). Regarding **2d** and **2g**, the latter concentration showed a 34% and 41% cell death.

Finally, AG1478 and the three pyrazolo-pyrimidines were compared for their ability to prevent phosphorylation of EGFR in cell stimulated with EGF at 10 ng ml^{-1}. At 1 μM, while AG1478 produced a 40% inhibition of EGFR phosphorylation, **2a, 2d**, and **2g** inhibited it by 25%, 18%, and 19%, respectively.

Compound **2a** was also investigated for its effects in the in vitro human EGF tyrosine kinase assay. As a result, an interesting 48% inhibition of control values obtained in the presence of **2a** was found, demonstrating that such a compound is an inhibitor of EGFR at its kinase site. The enzyme assay on EGF-TK was performed on A431 cells using PD153035 as the reference compound, according to the procedure reported by Carpenter et al. [29].

5. Conclusion

In conclusion, although compounds **2** did not show relevant A_1AR ligand activity, they may represent reasonable input structure to design and synthesize compounds with potential inhibitory activity toward tyrosine kinase receptors. Further efforts are ongoing in our labs to test the remaining compounds of the series **2**.

Moreover, it is important to point out that, to the best of our knowledge, **2a** is the first example of 6-substituted pyrazolo[3,4-*d*]pyrimidine showing anti-proliferative activity, probably acting on tyrosine kinase catalytic domain with possible anti-tumor applications.

6. Experimental protocols

6.1. Chemistry

Starting materials were purchased from Aldrich-Italia (Milan).

Melting points (m.p.) were determined with a Büchi B 540 apparatus and are uncorrected. IR spectra were recorded in KBr with a Perkin–Elmer 398 spectrophotometer. ^{1}H NMR spectra were recorded in $CDCl_3$ solution on a Varian Gemini 200 (200 MHz) instrument, chemical shifts (δ) are

[1] Cell proliferation was evaluated, as total cell number counted microscopically, after 24 h incubation with test compound in the presence of the specific growth factor. Cell cytotoxicity was evaluated by trypan blue exclusion following 1 h incubation with test compound. EC_{50} was calculated as the concentration of the compound able to give 50% of dead cells.

reported in ppm relative to TMS as internal standard; *J* in Hz. ^{1}H patterns are described using the following abbreviations: s, singlet; t, triplet; q, quartet; sext, sextet; m, multiplet; br, broad.

All compounds were tested for purity by TLC (Merk, Silica gel 60 F_{254}, $CHCl_3$ as eluant).

Analyses for C, H, N were within ±0.3% of the theoretical value.

*6.1.1. Ethyl 5-{[(benzoylamino)carbonothioyl]amino}-1-(2-hydroxy-2-phenylethyl)-1*H*-pyrazole-4-carboxylate (**4**)*

A suspension of **3** (2.7 g, 10 mmol) and benzoyl isothiocyanate (1.7 g, 11 mmol) in anhydrous tetrahydrofuran (20 ml) was refluxed for 12 h. The solvent was evaporated under reduced pressure; the oil residue crystallized adding diethyl ether (30 ml) to afford the pure product **4** (4.07 g, 93%) as a white solid, m.p. 171–172 °C. ^{1}H NMR: δ 1.29 (t, J = 7.0, 3H, CH_3), 3.97–4.20 (m, 5H, $2CH_2$ + OH, 1H disappears with D_2O), 4.58–4.68 (m, 1H, CHOH), 7.05–7.98 (m, 10H, Ar), 8.02 (s, 1H, H-3), 8.70 (s, 1H, NH, disappears with D_2O), 12.05 (s, 1H, NH, disappears with D_2O). IR (cm^{-1}): 3221 (NH), 3190–2940 (OH), 1708 and 1671 (2CO).

*6.1.2. 1-(2-Hydroxy-2-phenylethyl)-6-thioxo-1,5,6,7-tetrahydro-4*H*-pyrazolo[3,4-*d*]pyrimidin-4-one (**5**)*

A solution of **4** (4.38 g, 10 mmol) in 2 M NaOH (40 ml) was refluxed for 10 min and successively diluted with H_2O (40 ml). The solution was acidified with glacial acetic acid. Standing in a refrigerator for 12 h a solid crystallized, and was filtered and recrystallized from absolute ethanol to give **5** (2.3 g, 80%) as a white solid, m.p. 264–265 °C. ^{1}H NMR (d_6-DMSO): δ 4.15–4.30 and 4.55–4.72 (2m, 2H, CH_2N), 4.85–5.00 (m, 1H, CHO), 5.66 (br s, 1H, OH, disappears with D_2O), 7.20–7.51 (m, 5H, Ar), 8.02 (s, 1H, H-3), 12.20 (s, 1H, NH, disappears with D_2O), 13.40 (s, 1H, NH, disappears with D_2O). IR (cm^{-1}): 3362 (NH), 3142–2773 (OH), 1681 (CO).

*6.1.3. 1-(2-Hydroxy-2-phenylethyl)-6-(methylthio)-1,5-dihydro-4*H*-pyrazolo[3,4-*d*]pyrimidin-4-one (**6**)*

A solution of **5** (2.88 g, 10 mmol) and methyl iodide (7.10 g, 50 mmol) in anhydrous tetrahydrofuran (20 ml) was refluxed for 12 h. The solvent and the excess of methyl iodide were removed by distillation under reduced pressure; the oil residue crystallized by adding chloroform (10 ml) and was purified by recrystallization with absolute ethanol to give **6** (2.17 g, 72%) as a white solid, m.p. 208–209 °C. ^{1}H NMR: δ 2.51 (s, 3H, CH_3), 4.27–4.50 (m, 2H, CH_2N), 5.04–5.18 (m, 1H, CHO), 5.68 (d, 1H, OH, disappears with D_2O), 7.20–7.42 (m, 5H, Ar), 7.97 (s, 1H, H-3), NH not detectable. IR (cm^{-1}): 3544 (NH), 3450–3350 (OH), 1678 (CO).

*6.1.4. 4-Chloro-6-(methylthio)-1-(2-phenylvinyl)-1*H*-pyrazolo[3,4-*d*]pyrimidine (**7**)*

$POCl_3$ (14 g, 91 mmol) was added to **6** (3.02 g, 10 mmol), the mixture was refluxed for 12 h and then cooled to room temperature.

The excess of $POCl_3$ was removed by distillation under reduced pressure. H_2O (20 ml) was carefully added to the residue and the suspension was extracted with $CHCl_3$ (3 × 20 ml). The organic solution was washed with H_2O (10 ml), dried ($MgSO_4$), filtered and concentrated under reduced pressure. The crude brown oil was purified by column chromatography (Florisil® 100–200 Mesh), using $CHCl_3$ as eluant to afford the pure product **7** (0.9 g, 30%)) as a white solid, m.p. 108–109 °C. ^{1}H NMR: δ 2.70 (s, 3H, CH_3), 7.25–7.58 (m, 6H, 5H, Ar + 1H, CH=), 7.96 (d, J = 14.0, 1H, CH=), 8.14 (s, 1H, H-3). IR (cm^{-1}): 1658 (C=C).

*6.1.5. 4-Chloro-1-(2-chloro-2-phenylethyl)-6-(methylthio)-1*H*-pyrazolo[3,4-*d*]pyrimidine (**8**)*

The Vilsmeier complex, previously prepared from $POCl_3$ (6.13 g, 40 mmol) and anhydrous DMF (2.92 g, 40 mmol) was added to a suspension of **6** (3.02 g, 10 mmol) in $CHCl_3$ (20 ml).

The mixture was refluxed for 4 h. The solution was washed with H_2O (2 × 20 ml), dried ($MgSO_4$), filtered and concentrated under reduced pressure. The crude oil was purified by column chromatography (Silica gel, 100 Mesh), using a mixture of diethyl ether/petroleum ether (b.p. 40–60 °C) 1/1 as eluant, to afford the pure product **8** (2.2 g, 65%) as a white solid, m.p. 95–96 °C. ^{1}H NMR: δ 2.62 (s, 3H, CH_3), 4.77–5.05 (m, 2H, CH_2N), 5.45–5.56 (m, 1H, CHCl), 7.29–7.46 (m, 5H, Ar), 8.02 (s, 1H, H-3).

*6.1.6. General procedure for 1-(2-chloro-2-phenylethyl)-6-methylthio-1*H*-pyrazolo[3,4-*d*]pyrimidines 4-amino substituted (**2a–m**)*

To a solution of **8** (3.4 g, 10 mmol) in anhydrous toluene (20 ml), the proper amine (40 mmol) was added, and the reaction mixture was stirred at room temperature for 24 h. After it was extracted with H_2O, the organic phase was dried under reduced pressure; the oil residue crystallized by adding a mixture of diethyl ether/petroleum ether (b.p. 40–60 °C) 1/1 (5 ml), to give products **2a–m**.

Compound **2a**: White solid, m.p. 132–133 °C, yield 75%. ^{1}H NMR: δ 0.69–0.81 (m, 2H, CH_2), 0.92–1.08 (m, 2H, CH_2), 2.57 (s, 3H, CH_3S), 2.86–2.99 (m, 1H, CH), 4.72–4.98 (m, 2H, CH_2N), 5.51–5.62 (m, 1H, CH–Cl), 5.81 (br s, 1H, NH, disappears with D_2O), 7.22–7.58 (m, 5H, Ar), 8.08 (s, 1H, H-3). IR (cm^{-1}): 3410 (NH).

Compound **2b**: White solid, m.p. 126–127 °C, yield 76%. ^{1}H NMR: δ 1.02 (t, J = 5.0, 3H, CH_3), 1.73 (sext, J = 5.0, 2H, CH_2), 2.58 (s, 3H, CH_3S), 3.55 (q, J = 5.0, 2H, CH_2NH), 4.70–4.97 (m, 2H, CH_2N), 5.20 (br s, 1H, NH, disappears with D_2O), 5.49–5.58 (m, 1H, CHCl), 7.25–7.47 (m, 5H, Ar), 7.78 (s, 1H, H-3). IR (cm^{-1}): 3414 (NH).

Compound **2c**: White solid, m.p. 106–107 °C, yield 45%. ^{1}H NMR: δ 0.97 (t, J = 7.0, 3H, CH_3), 1.33–1.84 (m, 4H, $2CH_2$), 2.57 (s, 3H, CH_3S), 3.59 (q, J = 7.0, 2H, CH_2NH), 4.70–4.95 (m, 2H, CH_2N), 5.49–5.60 (m, 1H, CH–Cl), 7.23–7.49 (m, 5H Ar), 7.78 (s, 1H, H-3), NH not detectable. IR (cm^{-1}): 3413 (NH).

Compound **2d**: White solid, m.p. 80–81 °C, yield 50%. ^{1}H NMR: δ 1.57 (s, 9H, *t*-but), 2.61 (s, 3H, CH_3S), 4.68–4.98 (m, 2H, CH_2N), 5.08 (br s, 1H, NH disappears with D_2O), 5.51–5.62 (m, 1H, CHCl), 7.28–7.50 (m, 5H Ar), 7.73 (s, 1H, H-3).

Compound **2e**: White solid, m.p. 91–92 °C, yield 80%. ^{1}H NMR: δ 1.29 (t, J = 9.0, 6H, $2CH_3$), 2.57 (s, 3H, CH_3S), 3.71 (q, J = 9.0, 4H, $2CH_2$), 4.68–4.98 (m, 2H, CH_2N), 5.53–5.63 (m, 1H, CHCl), 7.26–7.50 (m, 5H, Ar), 7.73 (s, 1H, H-3).

Compound **2f**: White solid, m.p. 115–116 °C, yield 68%. ^{1}H NMR: δ 1.21 (t, J = 7.0, 3H, CH_3), 2.56 (s, 3H, CH_3S), 3.53 (q, J = 7.0, 2H, OCH_2CH_3), 3.55–3.85 (m, 4H, $2CH_2$), 4.66–4.97 (m, 2H, CH_2N), 5.45–5.60 (m, 1H, CHCl), 5.72 (br s, 1H, NH, disappears with D_2O), 7.27–7.44 (m, 5H, Ar), 7.77 (s, 1H, H-3). IR (cm^{-1}): 3441 (NH).

Compound **2g**: White solid, m.p. 138–139 °C, yield 72%. ^{1}H NMR: δ 1.14–1.57, 1.70–1.89 and 2.01–2.18 (m, 11H cyclohexyl), 2.57 (s, 3H, CH_3S), 3.98 (br s, 1H, NH, disappears with D_2O), 4.69–4.98 (m, 2H, CH_2N), 5.50–5.61 (m, 1H, CHCl), 7.23–7.49 (m, 5H, Ar), 7.73 (s, 1H, H-3). IR (cm^{-1}): 3402 (NH).

Compound **2h**: White solid, m.p. 151–152 °C, yield 52%. ^{1}H NMR: δ 1.90–2.06 (m, 2H, CH_2), 2.07–2.23 (m, 2H, CH_2), 2.58 (s, 3H, CH_3S), 3.69–3.86 (m, 4H, 2 CH_2Npyrr), 4.70–4.97 (m, 2H, CH_2N), 5.54–5.62 (m, 1H, CHCl), 7.24–7.57 (m, 5H, Ar), 7.79 (s, 1H, H-3).

Compound **2I**: White solid, m.p. 94–95 °C, yield 60%. ^{1}H NMR: δ 1.60–1.82 (m, 6H, $3CH_2$pip), 2.57 (s, 3H, CH_3S), 3.82–3.98 (m, 4H, $2CH_2$Npip), 4.70–4.97 (m, 2H, CH_2N), 5.53–5.64 (m, 1H, CHCl), 7.28–7.49 (m, 5H, Ar), 7.81 (s, 1H, H-3).

Compound **2j**: White solid, m.p. 116–117 °C, yield 75%. ^{1}H NMR: δ 2.57 (s, 3H, CH_3S), 3.79–3.98 (m, 8H, $4CH_2$morph), 4.71–4.98 (m, 2H, CH_2N), 5.51–5.61 (m, 1H, CHCl), 7.26–7.49 (m, 5H, Ar), 7.82 (s, 1H, H-3).

Compound **2k**: White solid, m.p. 99–100 °C, yield 60%. ^{1}H NMR: δ 1.46–1.69 and 1.75–1.98 (2m, 8H, $4CH_2$), 2.57 (s, 3H, CH_3S), 3.73–3.99 (m, 4H, CH_2NCH_2), 4.69–4.96 (m, 2H, CH_2N), 5.52–5.63 (m, 1H, CHCl), 7.24–7.50 (m, 5H, Ar), 7.76 (s, 1H, H-3).

Compound **2l**: White solid, m.p. 142–143 °C, yield 81%. ^{1}H NMR: δ 2.58 (s, 3H, CH_3S), 4.70–4.94 (m, 4H, CH_2N + CH_2NH), 5.50–5.60 (m, 1H, CH–Cl), 7.24–7.96 (m, 10H, Ar), 7.72 (s, 1H, H-3), NH not detectable. IR (cm^{-1}): 3442 (NH).

Compound **2m**: White solid, m.p. 73–74 °C, yield 76%. ^{1}H NMR: δ 2.59 (s, 3H, CH_3S), 2.98 (q, J = 6.0, 2H, $CH_2C_6H_5$), 3.87 (q, J = 6.0, 2H, CH_2NH), 4.70–4.95 (m, 2H, CH_2N), 5.30 (br s, 1H, NH, disappears with D_2O), 5.50–5.60 (m, 1H, CHCl), 7.19–7.48 (m, 10H Ar), 7.73 (s, 1H, H-3). IR (cm^{-1}): 3445 (NH).

6.2. Computational details

All calculations and graphical manipulations were performed on a Silicon Graphics Octane workstation and Origin 300 server using the software package MacroModel/BatchMin [17] equipped with the AMBER* united-atom force field.

The enzyme models used in this study were derived from the coordinates of the structure labeled 1m17 in the Brookhaven Protein Data Bank, which represent the complexes between the kinase domain of EGFR and a 4-anilinoquinazoline inhibitor (erlotinib), refined to 2.6 Å resolution.

To create initial coordinates for the docking studies, all the water molecules of the crystal structure were removed and excluded from the calculations. Similarly the 40 amino acids from the carboxy terminal tail of the EGFR structure were deleted. Hydrogen atoms were added in their idealized positions in such a way as to protonate all Lys and Arg side chains and deprotonate all Glu and Asp side chains.

In the present study, the computational step corresponding to the molecular docking approach is simplified, since the functional groups of the substrates interacting with the enzyme and the amino acid residues of the catalytic machinery are well known in advance. Thus, the docking problem is essentially reduced to locate the possible conformations of the ligand within the active site of the enzyme. The pyrimidine ring in the X-ray crystal structures was used to guide the building of the EGFR–**2a** complex providing a good template to adjust torsional angles of the inhibitor. In particular, the 4-aminopyrimidine ring of **2a** was superposed onto the corresponding ring of erlotinib.

In a second attempt, following the Traxler's model, **2a** was located into the binding site in such a way as to contact (with its endocyclic nitrogen atom at the 5-position and the secondary amino group at the 4-position) by hydrogen bonds the amide NH group of Gln767 and the carbonyl group of Met769, respectively.

The complexes generated were then submitted to a statistical conformational search with MCMM method involving the rotatable bonds of the inhibitor. MCMM causes an input structure to be modified by random changes in its torsion angles as given by the TORS command. Values of 0° and 180° are, respectively, the minimum and maximum angular increments to be added or subtracted from the current dihedral angles. It is important to note that conformational mobility of the active site residues was not a complicating factor since it has been shown that these residues undergo only minor structural changes upon the binding of different inhibitors [23].

The least square superimposition routine was selected (COMP command) to compare each new complex with all conformers previously found in order to eliminate duplicate minima.

Because of the large number of atoms in the model, to correctly optimize the EGFR–**2a** complexes, the following constraints had to be imposed: (a) a subset, centered on the inhibitor and comprising only the small molecules and a shell of residues surrounding the binding site of the enzyme within a radius of 10 Å from the ligand, was created and subjected to

energy minimization. The inhibitor and all amino acid side chains of the shell were unconstrained during energy minimization to allow for reorientation and thus proper hydrogen-bonding geometries and vdW contacts; (b) all the atoms external to the subset remained fixed, even if their non-bond interactions with all the relaxing atoms have been calculated.

Two intramolecular distances were monitored during the docking experiments in order to ensure that the relative orientations of the residues of the binding site remained compatible with the postulated interaction pattern. These were the distances between the amide hydrogen atom Met769 and the N5 atom of the pyrimidine ring of **2a**, and between the carbonyl oxygen atom of Gln767 and the hydrogen atom of the secondary amino group at the 4-position of **2a**.

Energy minimization of the complexes was performed using the Polak–Ribière conjugate gradient method until the derivative convergence was 0.01 kcal $Å^{-1}$ mol^{-1}. The default non-bonded cutoff protocol employed by the program was modified. Thus, a vdW cutoff of 12.0 Å, an electrostatic cutoff of 20 Å, and a hydrogen bonding cutoff of 2.5 Å were utilized for all calculations.

6.3. Biological

6.3.1. A_1 and A_{2A} adenosine receptor binding assays

[^{3}H]CHA, [^{3}H]CGS 21680 were obtained from DuPont-NEN (Boston, MA). DPCPX was purchased from RBI (Natik, MA). Adenosine deaminase was from Sigma Chemical Co. (St. Louis, MO). All other reagents were from standard commercial sources and of the highest commercially available grade.

Displacement of [^{3}H]CHA (31 Ci $mmol^{-1}$) from A_1AR in bovine cortical membranes and of [^{3}H]CGS 21680 (42.1 Ci $mmol^{-1}$) from A_{2A}AR in bovine striatal membranes was performed as described [24] Adenosine A_1 receptor affinities with [^{3}H]DPCPX as radioligand were determined according to Pirovano et al. [25]. Measurements with [^{3}H]DPCPX were performed in the presence and in the absence of 1 mM GTP.

Incubations were carried out in duplicate for 90 min at 25 °C. Non-specific binding was determined in the presence of 50 M R-PIA and constituted approximately 30% of the total binding. Binding reaction was terminated by filtration through a Whatman GF/C filter, washing three times with 5 ml of ice-cold buffer.

All compounds were routinely dissolved in DMSO and diluted with assay buffer to the final concentration, where the amount of DMSO never exceeded 2%.

At least six different concentrations spanning three orders of magnitude, adjusted appropriately for the IC_{50} of each compound, were used. IC_{50} values, computer-generated using a non-linear regression formula on a computer program (GraphPad, San Diego, CA), were converted to K_i values, knowing the K_d values of radioligands in the different tissues and using the Cheng and Prusoff equation [26]. The dissociation constant (K_d) of [^{3}H]CHA and [^{3}H]CGS 21680 were 1.2 and 14, respectively.

6.3.2. Inhibitory activity on cell proliferation

6.3.2.1. Cell lines and culture conditions. Cell culture reagents and materials were from Sigma Chemical Co. FCS was from Hyclone, Logan, UT, USA. Human recombinant EGF was from Calbiochem-Novabiochem Int., San Diego, CA, USA. Diff-Quik was from Mertz-Dade AG, Dudingen, Switzerland.

The human epidermoid carcinoma A-431 cells were obtained from American Type Culture Collection (Rockville, MD). A-431 cells were maintained in culture in DMEM supplemented with 4500 g l^{-1} glucose and 10% FCS. Cells were split 1:5 twice a week.

6.3.2.2. Cytotoxicity. The cytotoxic effect of compounds was evaluated by trypan blue exclusion. Cells were stimulated for 1 h at 37 °C with the increasing concentrations (10 nM–10 μM) of the test compound in 1% FCS medium. Cells were then stained with 0.4% trypan blue in phosphate buffer saline (PBS) for 5 min. The number of dead and living cells was counted at the microscope in a blind manner. The percentage of dead cells over the total number of cells was calculated.

6.3.2.3. Proliferation studies. Cell proliferation was quantified by total cell number as reported [27]. The compounds were tested at concentration ranging from 10 nM to 10 μM in the absence and in the presence of the growth factors EGF 0.1 pM, for 24 h.

6.3.2.4. Autophosphorylation assay. A-431 cells (3×10^6) were seeded in a 10 cm plate with 10% serum at 37 °C overnight and starved for 24 h, after which they were exposed to 1 μM of **2a, 2d, 2g** or AG1478 for 2 h and subsequently treated with 10 ng ml^{-1} EGF for 10 min at 37 °C. Proteins were extracted and 80 μg of lysate for each experimental point were subjected to 10% SDS-polyacrilamide gel electrophoresis and transferred to a PDVF membrane. Western blot analysis was performed as described [28]. The anti-phosphotyrosine antibody 1:2000 (Upstate Biotechnology) or anti-EGFR (Upstate Biotechnology) for the determination of corresponding receptor levels were incubated with the membranes for 18 h. Blots were incubated with HRP-goat anti-mouse antibody (Upstate Biotechnology) and the bands visualized with an enhanced chemiluminescence system (Amersham Pharmacia Biotech). Band intensities were measured using the ScioImage software package.

6.3.2.5. Human EGF tyrosine kinase assay. The experimental conditions are based on scintillation counting of the reaction product ([γ-^{33}P]poly GAT) obtaine d by combination of substrate/tracer (poly GAT, 0.48 mg ml^{-1}, and [γ-^{33}P]ATP) during a 60 min incubation at 30 °C. Results are expressed as percent inhibition of control values obtained in the presence of **2a**.

Acknowledgements

Financial support from Italian MIUR (Cofin 2002, prot. 2002038577_002) is gratefully acknowledged. The study was partially supported by funds from AIRC (Lucia Morbidelli). We are grateful to Sandra Donnini for technical assistance in the biological evaluation.

References

[1] J.W. Daly, J. Med. Chem. 25 (1982) 197–207.
[2] C.E. Müller, T. Scior, Pharm. Acta Helv. 68 (1993) 77–111.
[3] K.A. Jacobson, P.J.M. Van Galen, M. Williams, J. Med. Chem. 35 (1992) 407–422 (and references cited therein).
[4] A. Erfurth, M. Schmauss, Fortschr. Neurol. Psychiatr. 63 (1995) 93–98.
[5] P.J. Scammells, S.P. Baker, A.R. Beauglehole, Bioorg. Med. Chem. 6 (1998) 1517–1524.
[6] M. Williams, Med. Res. Rev. 9 (1989) 219–243.
[7] S.A. Poulsen, R. Quinn, Bioorg. Med. Chem. 6 (1998) 619–641.
[8] J.W. Daly, K.D. Hutchinson, S.I. Secunda, D. Shi, W.L. Padgett, M.T. Shamin, Med. Chem. Res. 4 (1994) 293–306.
[9] S. Psychoyos, C.J. Ford, M.A. Phillips, Biochem. Pharmacol. 31 (1982) 1441–1442.
[10] H.W. Hamilton, D.F. Ortwine, D.F. Worth, J.A. Bristol, J. Med. Chem. 30 (1987) 91–96.
[11] L.P. Davies, S.C. Chow, J.H. Skerrit, D.J. Brown, G.A.R. Johnston, Life Sci. 34 (1984) 2117–2128.
[12] S.A. Poulsen, J.R. Quinn, J. Med. Chem. 39 (1996) 4156–4161.
[13] F.A. Harden, J.R. Quinn, P.J. Scammells, J. Med. Chem. 34 (1991) 2892–2898.
[14] V. Ralevic, G. Burnstock, Pharmacol. Rev. 50 (1998) 413–492.
[15] G. Biagi, I. Giorgi, O. Livi, F. Pacchini, P. Rum, V. Scartoni, B. Costa, M.R. Mazzoni, L. Giusti, Farmaco 57 (2002) 221–233.
[16] F. Da Settimo, G. Primofiore, S. Taliani, A.M. Marini, C. La Motta, E. Novellino, G. Greco, A. Lavecchia, L. Trincavelli, C. Martini, J. Med. Chem. 44 (2001) 316–327.
[17] S. Schenone, O. Bruno, P. Fossa, A. Ranise, G. Menozzi, L. Mosti, F. Bondavalli, C. Martini, L. Trincavelli, Bioorg. Med. Chem. Lett. 11 (2001) 2529–2531.
[18] F. Bondavalli, M. Botta, O. Bruno, A. Ciacci, F. Corelli, P. Fossa, A. Lucacchini, F. Manetti, C. Martini, G. Menozzi, L. Mosti, A. Ranise, S. Schenone, A. Tafi, L. Trincavelli, J. Med. Chem. 45 (2002) 4875–4887.
[19] M. Chebib, J.R. Quinn, Bioorg. Med. Chem. 5 (1997) 311–322.
[20] S.A. Poulsen, D.J. Young, J.R. Quinn, Bioorg. Med. Chem. Lett. 11 (2001) 191–193.
[21] S. Schenone, O. Bruno, F. Bondavalli, et al., Abstract of Papers, 16th National Meeting of the Italian Chemical Society, Pharmaceutical Division, Sorrento, Italy, 18–22 September 2002.
[22] P. Traxler, G. Bold, J. Frei, M. Lang, N. Lyndon, H. Mett, E. Buchdunger, T. Meyer, M. Mueller, P. Furet, J. Med. Chem. 40 (1997) 3601–3616.
[23] J. Stamos, M.X. Sliwkowski, C. Eigenbrot, J. Biol. Chem. 277 (2002) 46265–46272.
[24] V. Colotta, D. Catarzi, F. Varano, L. Cecchi, G. Filacchioni, C. Martini, L. Trincavelli, A. Lucacchini, J. Med. Chem. 43 (2000) 1158–1164.
[25] I.M. Pirovano, A.P. Ijzermann, P.J. van Galen, W. Soudijn, Eur. J. Pharmacol. 172 (1989) 185–193.
[26] Y. Cheng, W.H. Prusoff, Biochem. Pharmacol. 22 (1973) 3099–3108.
[27] M. Ziche, L. Morbidelli, R. Choudhuri, H.T. Zhang, S. Donnini, H.J. Granger, R.J. Bicknell, Clin. Invest. 99 (1997) 2625–2634.
[28] Q. Qiu, F. Dudouit, S. Matheson, F. Brahimi, R. Banerjee, P. McNamee, B. Jean-Claude, Cancer Chemother. Pharmacol. 51 (2003) 1–10.
[29] G. Carpenter, L. King Jr, S. Cohen, J. Biol. Chem. 254 (1979) 4884–4891.